Rare Metal Materials and Engineering
Volume 49, Issue 8, August 2020
Available online at www.rmme.ac.cn

Science Press

Cite this article as: Rare Metal Materials and Engineering, 2020, 49(8): 2665-2673.

ARTICLE

Effect of Refinement and Modification on Microstructure, Properties and Eutectic Silicon Growth Mechanism of Cast A356 Aluminum Alloy

Wang Zhengjun, Zhang Qiuyang, Zhang Man, Liu Jingjing, Lv Jianqiang

Huaiyin Institute of Technology, Huai'an 223003, China

Abstract: The microstructures, mechanical properties and eutectic silicon growth mechanism of A356 aluminum alloy treated by novel Al-5Ti-1B-1RE and Al-10Sr master alloy with individual or composite refinement and modification were studied. The results show that under individual addition condition, the Al-5Ti-1B-1RE master alloy has a significant refinement effect on α-Al phase in A356 aluminum alloy and the tensile strength σ_b, yield strength σ_s and Vickers hardness of the alloy are significantly improved. Al-10Sr master alloy has a strong modification effect on eutectic silicon, and the elongation δ of the alloy is obviously improved. Under composite addition condition, the shape and size of α-Al phase in A356 aluminum alloy become more uniform and finer, and the grain boundaries are clearer. The eutectic silicon phases are almost converted into dispersed, fine fibrous shape, and the lamellar eutectic silicon almost completely disappears. The length of the eutectic silicon is reduced from 40~60 μm of the as-cast state to 1~2 μm, achieving a complete modification effect. Its mechanical properties are much higher than those of the as-cast, any single refiner and modifier treated A356 aluminum alloy. The growth mode of eutectic Si in the unrefined and unmodified A356 aluminum alloy is typical small-plane step growth. The eutectic silicon with composite refinement and modification is mainly grown by the twin plane re-entrant edge mechanism, and the growth characteristics of the facet are gradually weakened until disappearance.

Key words: refinement and modification; A356 alloy; microstructures and mechanical properties; small plane step growth; twin plane re-entrant edge mechanism

In virtue of their high specific strength, good castability and excellent corrosion resistance, Al-Si-Mg alloys have been widely applied in aerospace, construction and automobile industries[1-5]. A356 alloy is a hypoeutectic Al-Si-Mg alloy developed in the United States in the 1970s. Due to its excellent casting properties and outstanding comprehensive mechanical properties, it began to be widely used in automotive industry shortly after its appearance. However, the strength of cast A356 aluminum alloy is not high, especially elongation is very low[6,7]. Researchers have done a lot of research[8-12], and put forward a variety of theories and research methods. Among them, refinement and modification is the most widely used and most successful technology, and the technology is environment-friendly, easy to operate and so on[13]. As far as single refinement and modification of Al-Si alloy is concerned, there are many alternative process methods or types, but there are not many reports on the simultaneous refinement and modification for Al-Si alloy, especially for A356 aluminum alloy[14,15]. Considering operability and economy, and in order to achieve better synergy of refinement and modification effect, the self-made Al-5Ti-1B-1RE and Al-10Sr master alloy were used to composite refine and modify A356 aluminum alloy. Combining refinement and modification, A356 aluminum alloy was subjected to improving microstructure and mechanical properties. As the morphology of eutectic silicon was crucial to mechanical properties of the alloy, the growth mechanism of eutectic silicon was further explored. Through research and analysis of

Received date: August 16, 2019
Foundation item: National Natural Science Foundation of China (51701079); Doctoral Scientific Research Start-up Foundation from Huaiyin Institute of Technology, Jiangsu, China (Z301B18558)
Corresponding author: Wang Zhengjun, Ph. D., Associate Professor, Faculty of Mechanical and Material Engineering, Huaiyin Institute of Technology, Huai'an 223003, P. R. China, E-mail: wangzj2005@163.com

growth mechanism of eutectic silicon, the actual production practice can be guided. The properties and potential of the alloy can be fully improved and tapped, so that alloy materials with better properties can be produced and a certain theoretical basis can be laid for expanding industrial application.

1 Experiment

The experimental materials are mainly A356 aluminum alloy (Si 7.02 wt%, Mg 0.30 wt%, Fe 0.17 wt%, Al being the balance), the self-made Al-5Ti-1B-1RE master alloy[16], Al-10Sr mater alloy, special covering agent for aluminum and aluminum alloy, high purity argon gas (degassing), refining agent, paint, JJ-1 precision dynamoelectric stirrer and other auxiliary materials. When alloy element ingredients were calculated, the upper limit value of burning loss was taken for alloy elements with high burning loss rate.

The graphite crucible containing four equal parts of A356 aluminum alloy was placed in four KSL-12-JY well-type resistance furnaces with identical conditions and was heated to 730 °C. After the alloy became soft and concave, 0.50% aluminum alloy special covering agent was sprinkled on the surface (covering the heating components contained in the flux, stripping aluminum and aluminum oxide inclusions (Al_2O_3) and returning aluminum to the alloy liquid, and the slag was in powder form. The alloy liquid was effectively separated from the crucible wall and molten slag and the loss of aluminum alloy was reduced). After it was completely melted, refining and degassing were carried out. The removal of gas was carried out by rotary injection of high purity argon, which caused the molten aluminum to roll, resulting in "physical vibration", which caused the bubbles to escape (the technological parameters: revolutions 180 r/min, gas flow rate 1.8 L/min, degassing time 3 min, the same below). Strong stirring was carried out for 1 min by JJ-1 precision dynamoelectric stirrer, cooling to 710 °C, heat preservation for 5 min, slag removal and the melt in furnace 1 pouring. At the same time, a melt mass fraction of 0.80% the self-made Al-5Ti-1B-1RE master alloy refiner, 0.30% Al-10Sr master alloy modifier and the equivalent amount of both were pre-pressed into graphite bells in turn and added into the melts in furnace 2, furnace 3 and furnace 4, respectively. When adding a master alloy, the melts were strongly stirred by JJ-1 precision dynamoelectric stirrer for 1 min, followed by refining and degassing, then cooling to 710 °C, holding for 5 min, slag removal and pouring. The four groups above of the pouring rods were sawed laterally along the middle position in turn to prepare metallographic samples, and their microstructures were characterized by LEICA DM 2500 M transmission optical microscope and Hitachi S-3400 N scanning electron microscope. The Vickers micro-hardness test of the sample was carried out on HV-1000 micro-hardness tester (test conditions: during the test, the square conical diamond indenter with an included angle of 136° was pressed into the surface of the sample with a pressure of 4.90 kN and a holding time of 15 s). The above each poured test was repeated for three times, and each poured test rod was processed into standard tensile samples with 100 mm in gauge length according to the national standard GB/T 228.1-2010. Tensile mechanical properties were tested on an electronic universal experimental machine (CSS-44100) at a tensile rate of 1.00 mm/min. Each group of test data was average value of 3 tests.

2 Results and Discussion

2.1 Analysis of refiner and modifiers

The phase analysis of Al-5Ti-1B-1RE master alloy made by fusion method was carried out. The XRD pattern of the master alloy shows that the second phase particles are mainly Al_3Ti, TiB_2 and $Ti_2Al_{20}RE$ phases, as shown in Fig.1a. According to scanning electron microscopy and energy spectrum analysis, as shown in Fig.2a, the material with obvious edges and corners is Al_3Ti phase, as shown in point A. The massive material with slightly larger size and whitish surface edge was $Ti_2Al_{20}RE$ phase, as shown in point B. The fine black particulate matter is TiB_2 phase, as shown in point C. XRD analysis of Al-10Sr master alloy shows that the second phase particles are mainly Al_4Sr, as shown in Fig.1b. The gray bulky plate-like compound in Fig.2b, such as point D, analyzed by scanning electron microscope (SEM) and energy spectrum, is Al_4Sr phase, as shown in Fig.3a. The gray fine strip clusters

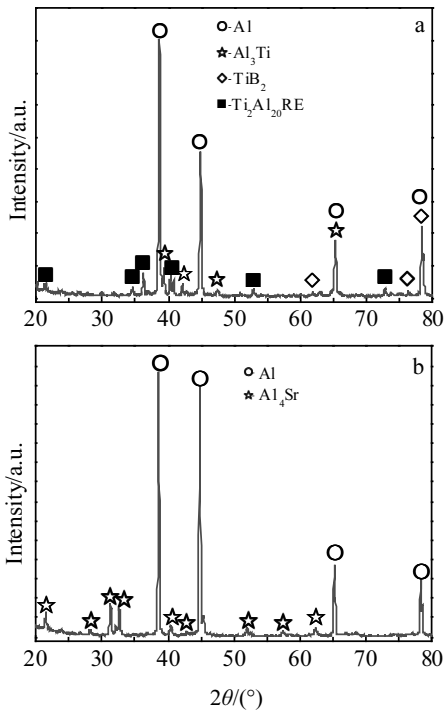

Fig.1 XRD patterns of Al-5Ti-1B-1RE (a) and Al-10Sr (b) master alloy

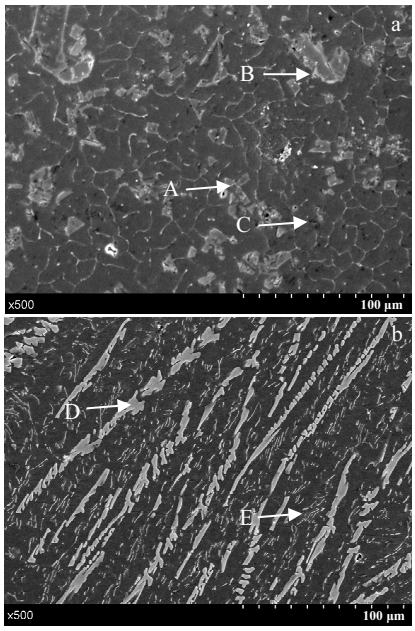

Fig.2 SEM micrographs of Al-5Ti-1B-1RE (a) and Al-10Sr (b)

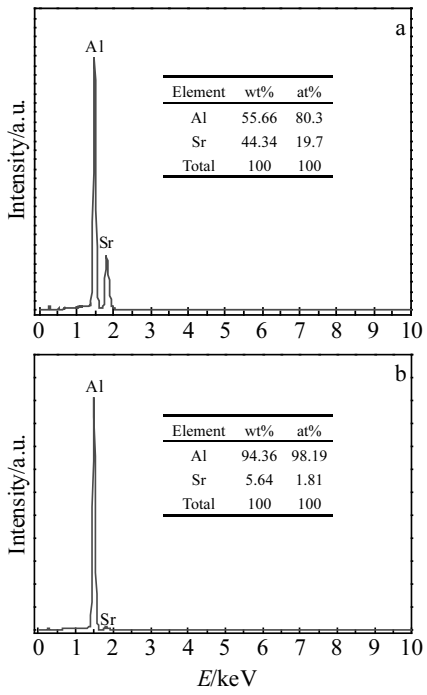

Fig.3 EDS spectra of Al-10Sr: (a) point D and (b) point E in Fig.2b

on the substrate in Fig.2b, such as point E, analyzed by scanning electron microscope energy spectrum, as shown in Fig.3b, is eutectic phase (Al+Al_4Sr).

2.2 Effect of refinement and modification on grain size of *α*-Al phase

The microstructure and morphology distribution of the four groups of A356 aluminum alloys treated by different processes are obviously different. When the optical microscope is at a low magnification, the coarse dendritic *α*-Al phase can be clearly observed, and the primary and secondary dendrites are not obvious, as shown in Fig.4a, which shows the A356 aluminum without alloy refinement and modification.

When 0.80% self-made Al-5Ti-1B-1RE master alloy refiner and modifier is added, the shape and size of *α*-Al phase become more uniform and finer, closely arranged, regular in shape, clear in grain boundary, and the secondary dendrites are greatly reduced, mainly with fine and dense equiaxed crystal structure, as shown in Fig.4b, which shows that self-made Al-5Ti-1B-1RE master alloy not only has obvious refining effect on industrial pure aluminum, but also has obvious refining effect on *α*-Al in aluminum alloy. This significantly expands the application range of Al-5Ti-1B-1RE master alloy. And the Vickers microhardness values of several random tests are basically equal, indicating that there are almost no needle holes in the tested places. It could be seen that Al-5Ti-1B-1RE master alloy refiner has remarkable grain refinement, degassing and deslagging functions, and contains a large number of Al_3Ti, TiB_2 and other second phase particles, which plays a dual nucleation and refinement role in the solidification process of aluminum liquid, increasing nucleation rate and refining grains. While the generated second phase particles $Ti_2Al_{20}RE$ phase first releases RE atoms in the aluminum melt, partially transforms into Al_3Ti, and then further dissolves. The whole process is similar to the occurrence of peritectic reaction, i.e. $L+Ti_2Al_{20}RE \rightleftharpoons \alpha\text{-Al(Ti)}+RE$, and releases rare earth elements with atomic radius of 0.174~0.204 nm, which is larger than aluminum atomic radius of 0.143 nm, and has extremely low solid solubility in aluminum[17]. The precipitated rare earth elements cause lattice distortion of *α*-Al and have pinning effect on grain boundaries so that grain boundaries cannot continue to grow, effectively playing a role in grain refinement. Therefore, the grain size of *α*-Al phase in A356 aluminum alloy refined and modified by Al-5Ti-1B-1RE master alloy becomes uniform and fine.

When 0.30% Al-l0Sr master alloy is added, i.e. Sr is 0.03%, the *α*-Al phase is refined to some extent, but it is basically in the shape of coarse columnar crystal, and the primary and secondary dendrite arms are more obvious (especially in the area marked by the blue ellipse in Fig.4c), which further proves that the aluminum alloy modified with Sr alone has limited the refinement to *α*-Al phase, mainly because a certain amount of Al_4Sr compounds are distributed in Al-l0Sr master alloy. Only when Sr in Al_4Sr compounds is only converted into free state, i.e. $Al_4Sr \rightleftharpoons 4Al+Sr$, can it play its role of refinement and modification. Therefore, the stability of Al_4Sr is the key factor to determine its refinement and modification effect, while the stability of Al_4Sr is closely related to its shape, size, distribution and other factors. In Fig.2b, such as point D, Sr atoms are not easy to dissociate from Al_4Sr and the

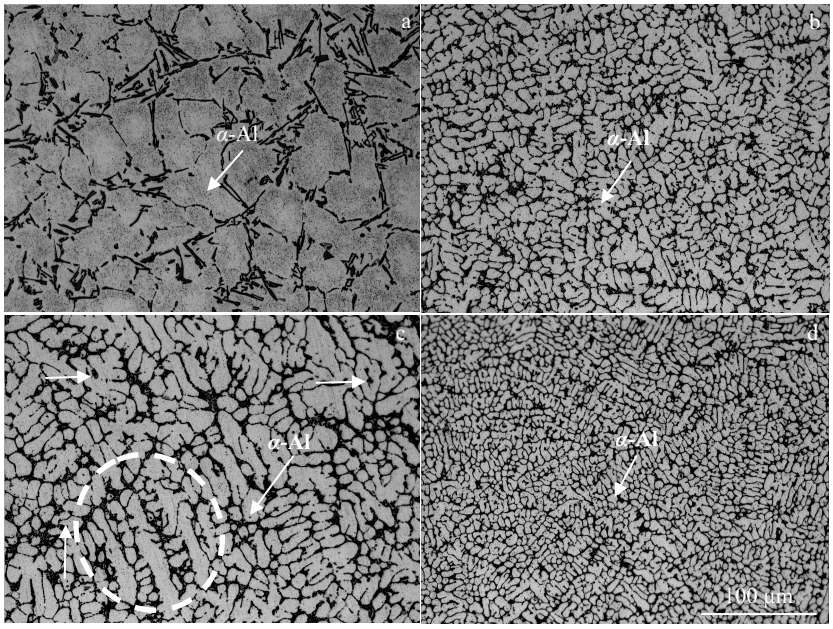

Fig.4 Morphologies of grain size of A356 alloy: (a) as-cast alloy, (b) with 0.80% Al-5Ti-1B-1RE, (c) with 0.30% Al-10Sr master alloy, and (d) with 0.80% Al-5Ti-1B-1RE and 0.30% Al-l0Sr

refinement and modification effect is poor, while for $A1_4Sr$ with fine dispersion, in Fig.2b, such as point E, due to its large specific surface area and high surface energy, its dissolution rate would be fast and Sr atoms are easy to dissociate from it and easily exert Sr refinement and modification effect. Due to a large number of coarse sheets $A1_4Sr$ in the A1-10Sr master alloy used in the test, a single Sr modification treatment fails to achieve a better α-Al phase refinement effect, and the melt has an obvious inspiratory tendency after Sr addition, as indicated by the red arrow in Fig.4c. The Vickers microhardness value is obviously lower than that in other regions. According to its morphological distribution characteristics, it can be determined as fine needle holes.

After adding 0.80% Al-5Ti-1B-1RE and 0.30% Al-l0Sr master alloy composite refiner and modifier, the α-Al phase becomes more uniform and finer in shape and size, closer in arrangement, regular in shape, clear in grain boundary, which is mainly small and dense equiaxed crystal structure, with almost no dendritic crystal structure, as shown in Fig.4d. The Vickers microhardness values of several random test samples are basically equal, and no pinholes are found in the test area. This indicates that the refining and modification effect of Al-5Ti-1B-1RE and Al-10Sr master alloy can be maximized, which not only significantly refines the α-Al phase in A356 aluminum alloy, but also greatly reduces the suction tendency of the melt.

2.3 Effect of refinement and modification on morphology of eutectic Si phase

The α-Al phase of A356 aluminum alloy unmodified is irregular in shape under high magnification optical microscope. The eutectic silicon is in the form of a thick plate or a long needle, with a large morphological difference, a dimension length of 40~60 μm, a width of 4~6 μm, and length-to-diameter ratio of more than 10. It has obvious facet growth characteristics. There is also no obvious interface between eutectic structure and primary α-Al, and the distribution in the aluminum matrix is non-directional, irregular, scattered, with sharp corners at the edges, as shown in Fig.5a. It is brittle and seriously affects the continuity of the matrix, breaking the matrix and causing stress concentration. The tensile strength, yield strength, elongation and Vickers hardness are 177.56 MPa, 110.44 MPa, 1.17% and 725.0 MPa, respectively. According to the test result, the mechanical properties are not high.

When 0.80% Al-5Ti-1B-1RE master alloy is added alone, the shape and size of α-Al phase become uniform and fine, grain boundaries are clear. The grain refinement effect is obvious. The distribution of eutectic silicon in the alloy becomes uniform, and the length and thickness of lamellar eutectic silicon are also significantly reduced, mostly in the form of short rods, but eutectic silicon still has a fine lamellar or blocky structure in some areas, which does not achieve a complete modification effect for eutectic silicon, as shown in Fig.5b. Its tensile strength, yield strength, elongation and Vickers hardness are 230.34 MPa, 160.08 MPa, 5.41% and 789.2 MPa, respectively, and its mechanical properties are obviously improved.

When 0.30% Al-10Sr master alloy is added alone, the α-Al phase has obvious grain boundaries and grain size is refined to

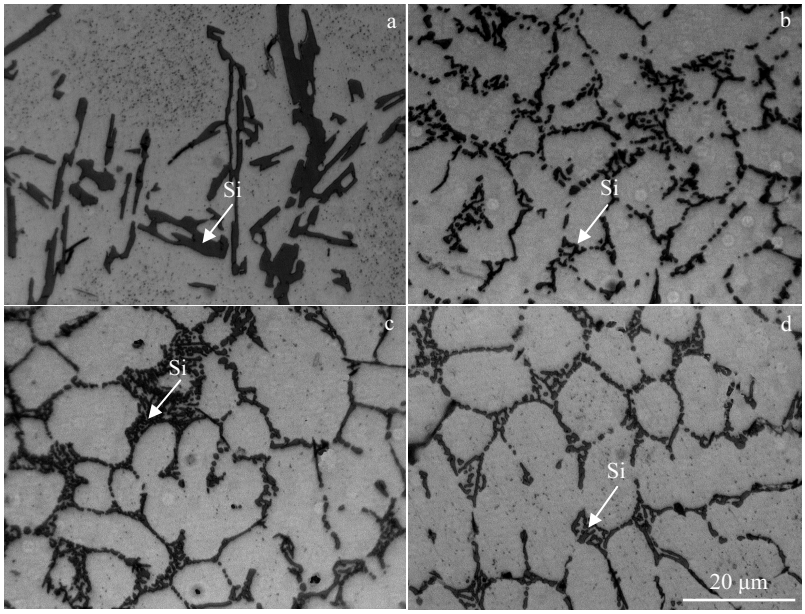

Fig.5 Microstructures of eutectic silicon of A356 alloy: (a) as-cast alloy, (b) with 0.80% Al-5Ti-1B-1RE, (c) with 0.30% Al-10Sr, and (d) with 0.80% Al-5Ti-1B-1RE and 0.30% Al-l0Sr

a certain extent, but the size is not uniform. Compared with unmodified eutectic silicon, the morphology of Sr-modified eutectic silicon has changed significantly, most of which have become fine fibrous structures, and a few of which are short rods with sizes below 10 μm, and the distribution is relatively concentrated, with highly branched eutectic silicon dendrites. At the same time, the interface between eutectic structure and matrix becomes smooth and flat after modification, as shown in Fig.5c. Its tensile strength, yield strength, elongation and Vickers hardness are 222.97 MPa, 147.38 MPa, 5.70% and 767.2 MPa, respectively, and its mechanical properties are significantly improved compared with those of A356 aluminum alloy without modification.

When Al-5Ti-1B-1RE and Al-l0Sr master alloy are all added, the shape and size of α-Al phase become more uniform and finer, and grain boundaries become clearer. The modification effect of eutectic silicon is better than that of any single refinement and modification. The eutectic silicon phases are almost all transformed into dispersed and fine fibers. The lamellar eutectic silicon almost completely disappears. The size of eutectic silicon reaches the minimum value, mostly between 1~2 μm, and the profile is clear, mainly uniformly distributed at grain boundaries to play the role of grain boundary strengthening, as shown in Fig.5d. According to the modification grade chart of hypoeutectic Al-Si alloy provided by the American Foundry Society (AFS) as the evaluation standard[18], the effect of composite refinement and modification of eutectic silicon is assessed to be grade 5 to achieve the complete modification grade. This is mainly because Sr has a very strong modifying effect on eutectic silicon, so that eutectic silicon is more evenly distributed in Al matrix of the soft tough phase. At the same time, introduction of rare earth elements has played a positive role in promoting Sr modification. Rare earth elements are adsorbed on the surface of silicon to inhibit the growth of the silicon phases, reduce the surface energy, and increase the wettability of the melt to the silicon phases[19]. The tensile strength, yield strength, elongation and Vickers hardness of the alloy are 242.06 MPa, 172.14 MPa, 6.54% and 811.4 MPa, respectively. Compared with those of as-cast A356 aluminum alloy, the tensile strength, yield strength, elongation and Vickers hardness of 356 aluminum alloy with composite refinement and modification are increased by 36.33%, 55.87%, 458.97% and 11.92%, respectively. Their mechanical properties are greatly improved, especially elongation, as shown in Fig.6.

2.4 Effect of refinement and modification on mechanical properties of A356 aluminum alloy

The refinement and modification effect of A356 aluminum alloy can be measured by the microstructure, for example, α-Al is refined or (and) the eutectic silicon phases are changed from flake to fibrous. On the other hand, it can also be measured by the mechanical properties of alloys before and after refinement and modification.

When 0.80% Al-5Ti-1B-1RE master alloy is added alone, the yield strength of A356 aluminum alloy (II) is 7.93% higher than that of A356 aluminum alloy (III) with 0.30% Al-l0Sr master alloy, but the elongation is 5.36% lower. The main reason is that the eutectic point of the alloy decreases after Sr modification and crystallization temperature range of the alloy increases[20], leading to full growth of primary α(Al) and

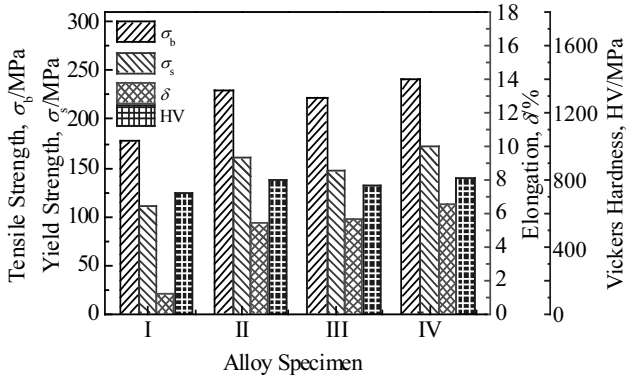

Fig.6 Mechanical properties of A356 aluminum alloys by different processes (I-as-cast alloy; II-with 0.80% Al-5Ti-1B-1RE; III-with 0.30% Al-10Sr; IV-with 0.80% Al-5Ti-1B-1RE and 0.30% Al-l0Sr)

increase of grain size of the final solidified structure, as shown in Fig.5c. Eutectic Si phase is mainly distributed at grain boundary, according to grain boundary fine grain strengthening theory and Hall-Petch relation[21]:

$$\sigma_s=\sigma_0+Kd^{1/2} \quad (1)$$

where, σ_s is yield strength, σ_0 is the initial strength of metal, d is the average size of the grain in polycrystal, and K is a constant showing the impact of grain boundary on the strength, which is related to the grain boundary structure, but little relevant with temperature. It can be seen from Eq. (1) that with the decrease of grain size d, mechanical properties of the alloy, especially yield strength increases.

As far as the elongation of the alloy is concerned, the improvement of A356 alloy (IV) after composite refinement and modification is mainly due to the essential transformation of the morphology of eutectic silicon compared with the other three different groups of A356 aluminum alloys. The size of eutectic silicon after composite refinement and modification is obviously reduced, and the morphology is mostly changed from coarse lamellar to fibrous and greatly reduced to split the matrix. When eutectic silicon is uniform and finely fibrous, the possibility of breaking itself will be significantly reduced, and the bonding strength with the matrix increases obviously, which improves the mechanical properties of the alloy.

2.5 Analysis of growth mechanism of eutectic Si

Al-5Ti-1B-1RE master alloy dual nucleation refinement theory[22] on the refining mechanism of pure aluminum is also applicable to α-Al phase in A356 aluminum alloy. However, the rare earth elements introduced by Al-5Ti-1B-1RE master alloy refiner not only promote the refining of α-Al phase, but also are adsorbed on the surface of silicon to inhibit the growth of silicon phase, reduce the surface energy, increase the wettability of melt to silicon phase, and refine and modify eutectic silicon in the form of a short rod or fiber, which play a positive role. However, under the same conditions, Al-10Sr master alloy is much stronger than Al-5Ti-1B-1RE master alloy in modifying eutectic silicon in A356 aluminum alloy, and the morphology of eutectic silicon in Fig.5c is better than that in Fig.5b, indicating that Sr plays a leading role in modifying eutectic silicon.

2.5.1 Growth mechanism of unmodified eutectic Si

The surface of the unmodified eutectic silicon is smooth, the morphology is plate-like, and almost no twins appear, as shown in Fig.7 by TEM analysis of the interface between unmodified eutectic silicon and aluminum matrix. Some studies have shown that two or more pairs of twins parallel to each other appeared, and the twin grooves can become the position of the silicon atoms that never disappeared[23]. However, the twin groove of a single twin would disappear after the silicon atoms are attached, which could not provide sufficient attachment sites for silicon atoms. As can be seen from Fig.7, neither single twin nor twin pairs are found on the eutectic silicon of the unmodified A356 aluminum alloy. At the same time, a large number of SEM and TEM analyses of unmodified eutectic Si show that there is at most one twin on the unmodified alloy eutectic Si, and no large angle branching angle of 70.5° is found. Therefore, the twin growth mechanism is not the main one for unmodified eutectic Si.

The Si phase protrudes from the front of the solid-liquid interface during eutectic two-phase growth in the unmodified A356 aluminum alloy. So, the analysis of Si crystal growth end shape can better reflect the crystal growth rule. The morphology of unmodified eutectic silicon is in the form of thick plate-like or long needle-like, lapping and overlapping with each other, with no obvious branching characteristics, but obvious convex corners at the growth tips and random distribution in the aluminum matrix, as shown in Fig.8a. At high magnification of the scanning electron microscope, the growth of unmodified eutectic Si is characterized by a small plane, a thick lamellar, and steps with arc-shaped concave angles as indicated by red arrow, less than 1 μm in height and relatively regular. This concave angle is a typical concave angle measured at about 50°, as shown in Fig.8b. These steps existing on unmodified eutectic Si are inherent, not accidental

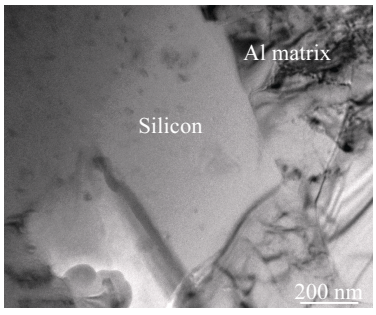

Fig.7 TEM image of interface of unmodified eutectic silicon and aluminum

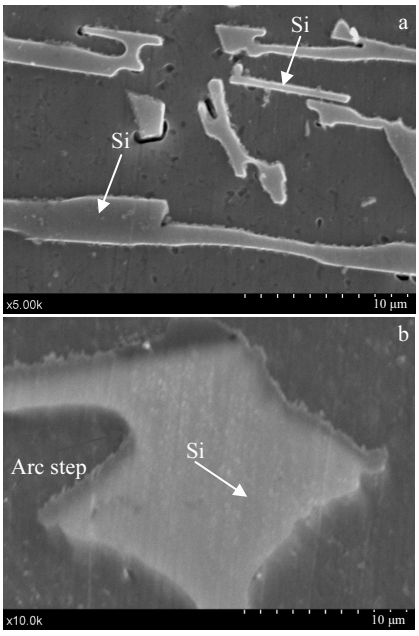

Fig.8 Microstructures of eutectic silicon in unmodified A356 alloy: (a) thick plate-like or long needle-like and (b) small plane-like

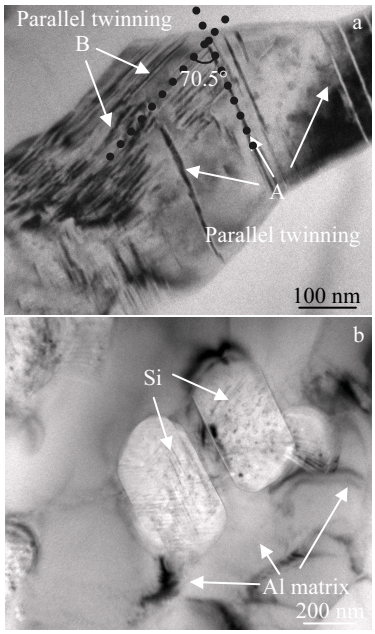

Fig.9 TEM images of twin morphology of eutectic silicon after modification: (a) high-density twins and (b) few twins

or caused by other reasons, and the presence of steps contributes to the growth of unmodified eutectic Si[24]. Therefore, the growth mode of unmodified eutectic Si belongs to typical facet step growth.

2.5.2 Growth mechanism of modified eutectic Si

As can be seen from Fig.9a, there are a large number of parallel twins at region A on eutectic silicon, and a group of parallel twins at region B appear on the upper left of the region A. The angle between parallel twins at region B and region A is 70.5°, which is the angle of large-angle branching caused by growth of eutectic silicon twins. After refinement and modification, the eutectic silicon exhibits typical "zigzag" morphology branches. It can be seen that the modified elements are adhered to the (111) close-packed surface of eutectic silicon to generate twins, and the concave angle formed by two (111) surfaces of twins provides a ready-made step for crystal growth. The modified atoms can be stacked directly at the root of the concave groove. When growth is carried out in the direction contained in the twin plane, the concave angle always exists, and thus ensuring continuous growth and eutectic silicon would change its growth direction due to the generation of twins[25]. There are two main reasons for the presence of high-density twins on eutectic silicon. Firstly, the solid-liquid interface structure of eutectic silicon is transformed by modification, and the small-plane growth mode of monatomic layer is gradually transformed into the non-small-plane growth mode of polyatomic layer. The small-plane characteristics of eutectic silicon are gradually weakened until disappearance. Secondly, the enrichment of the modified element Sr in the solid-liquid interface front of eutectic silicon increases, so the twin density of eutectic silicon also increases to a certain extent. More than two groups of parallel twins with an angle of 70.5° appear on eutectic silicon, which are typical "zigzag" growth. High-density twins appear in most of the eutectic silicon, as shown in Fig.9a, and few twins exist in a small number of granular eutectic silicon after modification, as shown in Fig.9b. However, the increase of twin density after modification provides a strong evidence for the mechanism of impurity-induced twins. The modified atoms induce twins, resulting in a high degree of branching of the eutectic silicon, eventually forming a fibrous structure[26].

The high-resolution image analysis of the intersecting region of the twins shows a secondary twin, as shown in Fig.10, marked by A and B. The spacing between the twin planes is about 16 nm and the twins cross each other at 70.5°. Compared with PDF card of Si, the two faces in the figure should be correspond to two (111) faces of Si. Si crystals (111) plane energy is the lowest, which is easy to produce twins, other plane defects and high branching structures, reduce the energy of crystal and make it more stable[27].

Fig.11 shows the morphological characteristics of eutectic Si after refinement and modification of Al-5Ti-1B-1RE and Al-10Sr master alloys. Eutectic Si with two-dimensional dispersed distribution can be observed in SEM high magnification images. But in fact, it is a coral-like three-dimensional shape that is connected together, as shown in Fig.11a. In the TEM image, it can be clearly seen that the morphology of eutectic Si has

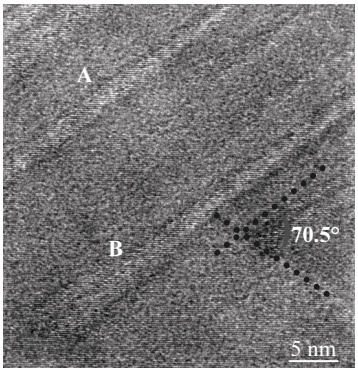

Fig.10 HRTEM image of twin in eutectic silicon

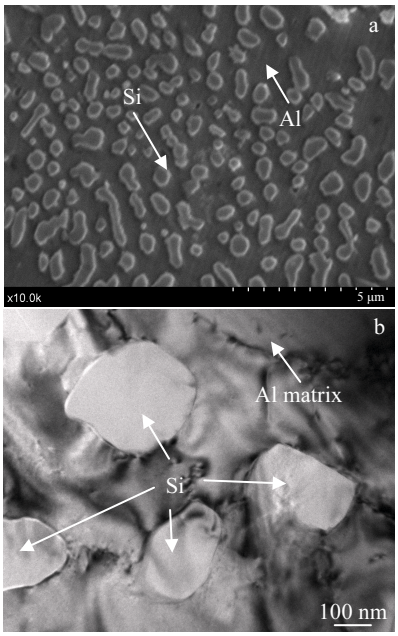

Fig.11 SEM (a) and TEM (b) morphologies of eutectic Si in modified A356 alloy with Al-5Ti-1B-1RE and Al-10Sr master alloys

changed significantly, and the growth characteristics of eutectic Si have changed from original anisotropy to isotropy. As a result, eutectic Si changes from coarse flake to fibrous before modification, resulting in a qualitative change in the morphology and size of eutectic Si[28], and the flake features disappear, showing granular characteristics at TEM image, as shown in Fig.11b.

The stacking fault energy of Al is 0.20 J/m^2, and that of Si is 0.046 J/m^2. The smaller the stacking fault energy, the greater the probability of stacking faults, that is, stacking defects are more prone to occur in eutectic silicon and the interior of the aluminum grains around the eutectic silicon is relatively clean, and substantially no crystal defects are generated in aluminum-silicon alloys, as shown in Fig.12. The

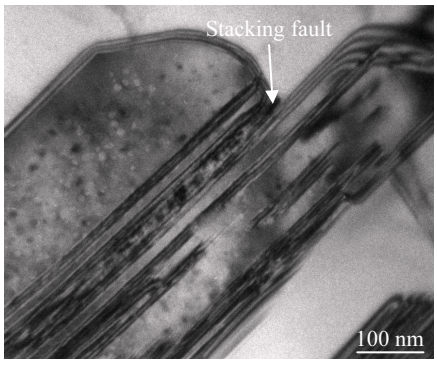

Fig.12 Stacking fault of eutectic Si fiber with defects

high-density stacking fault contributes greatly to the branching of eutectic Si, and the eutectic Si continues to grow by twin plane re-entrant edge (TPRE) mechanism after branching.

In summary, Sr is adsorbed on the front edge of the solid-liquid interface of eutectic silicon; therefore, it induces a large number of twins, and results in multiple and high branching of eutectic silicon, thus inhibiting the lateral growth of inherent steps, changing the growth direction and forming a fibrous structure. And with the increase of twin density to a certain extent, the small plane characteristics of eutectic silicon gradually weaken until disappearance. And the atomic radii of Sr and Si are r_{Sr}=2.160×10^{-10} m and r_{Si}=1.175×10^{-10} m, respectively, so the atomic radius ratio of Sr to Si is 1.838, which is close to the optimal atomic radius ratio (1.6475) of impurity-induced twin mechanism[25]. Therefore, the combination of these factors promotes the growth of modified eutectic Si by TPRE mechanism.

3 Conclusions

1) The self-made Al-5Ti-1B-1RE master alloy and Al-10Sr master alloy are used to refine and modify A356 aluminum alloy. The microstructure and mechanical properties of A356 aluminum alloy with composite refinement and modification treatment are greatly improved compared with those of treated with as-cast or any single one. Compared with those of as-cast A356 aluminum alloy, the tensile strength, yield strength, elongation and Vickers hardness of 356 aluminum alloy with composite refinement and modification are increased by 36.33%, 55.87%, 458.97% and 11.92%, respectively.

2) Few twins are found on eutectic silicon of unmodified A356 aluminum alloy. The growth mode of unmodified eutectic silicon belongs to typical small plane step growth.

3) The facet characteristics of the eutectic silicon treated by composite refinement and modification gradually weaken until disappearance. And more than two groups of parallel twins with an angle of 70.5° appear, which are typical “zigzag” growth, with a large number of twins occurring and growing by twin plane re-entrant edge mechanism.

References

1 Camicia G, Timelli G. *Transactions of Nonferrous Metals Society of China*[J], 2016, 26(5): 1211
2 Sun Huaping, Wu Jun, Tang Tian *et al*. *International Journal of Minerals, Metallurgy and Materials*[J], 2017, 24(7): 833
3 Esgandari B A, Nami B, Shahmiri M *et al*. *Transactions of Nonferrous Metals Society of China*[J], 2013, 23(9): 2518
4 Zhang Jie, Zhang Dongqi, Wu Pengwei *et al*. *Rare Metal Materials and Engineering*[J], 2014, 43(1): 47
5 Qiu Ke, Wang Richu, Peng Chaoqun *et al*. *Transactions of Nonferrous Metals Society of China*[J], 2015, 25(11): 3886
6 Zhang Junkai, Zhang Qin, Li Ying *et al*. *Rare Metal Materials and Engineering*[J], 2017, 46(1): 274
7 Hou Longgang, Liu Mingli, Wang Xindong *et al*. *Acta Metallurgica Sinica*[J], 2017, 53(9): 1075 (in Chinese)
8 Chen Rui, Shi Yufeng, Xu Qingyan *et al*. *Transactions of Nonferrous Metals Society of China*[J], 2014, 24(6): 1645
9 Xie Huanjun, Cheng Yingliang, Li Shaoxian *et al*. *Transactions of Nonferrous Metals Society of China*[J], 2017, 27(2): 336
10 Yang Changlin, Li Yuanbing, Dang Bo *et al*. *Transactions of Nonferrous Metals Society of China*[J], 2015, 25(10): 3189
11 Elahi M A, Shabestari S G. *Transactions of Nonferrous Metals Society of China*[J], 2016, 26(4): 956
12 Faccoli M, Dioni D, Cecchel S *et al*. *Transactions of Nonferrous Metals Society of China*[J], 2017, 27(8): 1698
13 Liu Zheng, Liu Xiaomei, Zhu Tao *et al*. *Acta Metallurgica Sinica*[J], 2015, 51(3): 272 (in Chinese)
14 Liu Zheng, Chen Qingchun, Guo Song *et al*. *Rare Metal Materials and Engineering*[J], 2015, 44(4): 859
15 Chen Xiang, Ghen Huiyuan, Li Yanxiang. *Acta Metallurgica Sinica*[J], 2006, 42(4): 1130 (in Chinese)
16 Wang Zhengjun, Si Naichao. *Rare Metal Materials and Engineering*[J], 2015, 44(12): 2970
17 Yang Huaide, Long Siyuan, Zhu Shuqing *et al*. *Rare Metal Materials and Engineering*[J], 2016, 45(1): 187
18 Chen Xiang, Ghen Huiyuan, Li Yanxiang. *Acta Metallurgica Sinica*[J], 2005, 41(8): 891 (in Chinese)
19 Liu Zheng, Xu Lina, Yu Zhaofu *et al*. *Acta Metallurgica Sinica*[J], 2016, 52(6): 698 (in Chinese)
20 Li Bao, Wang Hongwei, Wei Zunjie. *Journal of Wuhan University of Technology*[J], 2009, 24(S1): 47
21 Cui Zhongqi, Tan Yaochun. *Metallurgy and Heat Treatment*[M]. Beijing: China Machine Press, 2007: 175 (in Chinese)
22 Wang Zhengjun, Si Naichao. *Rare Metal Materials and Engineering*[J], 2015, 44(6): 1494 (in Chinese)
23 Nikitin V I, Jie W Q, Kandaloval E G *et al*. *Scripta Materialia*[J], 2000, 42(6): 561
24 Zhang Jing. *Thesis for Doctorate*[D]. Jinan: Shandong University, 2011 (in Chinese)
25 Li Bao. *Thesis for Doctorate*[D]. Harbin: Harbin Institute of Technology, 2011 (in Chinese)
26 Zu Fangqiu, Li Xiaoyun. *China Foundry*[J], 2014, 11(4): 287
27 Zhang J, Kang S B, Yu H S *et al*. *Materials and Design*[J], 2011, 32(6): 3566
28 Zu Fangqiu. *Foundry*[J], 2011, 60(11): 1073 (in Chinese)

细化变质处理对铸造 A356 铝合金组织性能及共晶硅生长机制的影响

王正军，张秋阳，张　满，刘静静，吕建强

(淮阴工学院，江苏 淮安 223003)

摘　要：研究采用新型 Al-5Ti-1B-1RE 中间合金和 Al-10Sr 中间合金对 A356 铝合金进行单一或复合细化变质处理后的组织、力学性能和共晶硅生长机制的影响。结果表明：单一细化变质处理中 Al-5Ti-1B-1RE 中间合金对 A356 铝合金中 α-Al 相有明显的细化作用，合金的强度和维氏硬度显著提高；Al-10Sr 中间合金对共晶硅有强的变质作用，合金的伸长率明显提高；而经复合细化变质处理后 α-Al 相形状和尺寸变得更均匀细小，晶界更清晰，片层状共晶硅也几乎完全消失，共晶硅相几乎都转变成更弥散、更细小的纤维状，共晶硅长度由铸态 40~60 μm 减小到 1~2 μm 之间，达到完全变质效果，其力学性能显著高于铸态、单一细化变质剂处理的 A356 铝合金。未细化变质的 A356 铝合金中的共晶 Si 的生长方式为典型的小平面台阶生长，复合细化变质处理的共晶硅以孪晶凹槽机制生长为主，小平面生长特征逐渐减弱直至消失。

关键词：细化变质；A356 铝合金；组织性能；小平面生长特征；孪晶凹槽生长机制

作者简介：王正军，男，1975 年生，博士，副教授，淮阴工学院机械与材料工程学院，江苏 淮安 223003，E-mail: wangzj2005@163.com